Molecular Crystals and Liquid Crystals Science and Technology. Section A. Molecular Crystals and Liquid Crystals

Publication details, including instructions for authors and subscription information:
http://www.tandfonline.com/loi/gmcl19

Effects of Composition on Thermo-Optical Properties of (Side Chain Smectic-A Liquid Crystalline Polymer/Low Molecular Weight Nematic Liquid Crystal/Chiral Dopant) Ternary Composite System

Huai Yanga [a], Hirokazu Yamane [b], Hirotsugu Kikuchi [b] & Tisato Kajiyama [b]

[a] Institute of Materials Science, Jilin University, Changchun, 130023, China

[b] Department of Chemical Science and Technology, Faculty of Engineering, Kyushu University, 6-10-1 Hakozaki, Higashi-ku, Fukuoka, 812, Japan

Version of record first published: 04 Oct 2006

Mol. Cryst. Liq. Cryst., 1998, Vol. 312, pp. 179 - 202
Reprints available directly from the publisher
Photocopying permitted by license only

Effects of Composition on Thermo-Optical Properties of (Side Chain Smectic-A Liquid Crystalline Polymer/Low Molecular Weight Nematic Liquid Crystal/Chiral Dopant) Ternary Composite System

HUAI YANG[a,*], HIROKAZU YAMANE[b], HIROTSUGU KIKUCHI[b] and TISATO KAJIYAMA[b]

[a] *Institute of Materials Science, Jilin University, Changchun, 130023, China;*
[b] *Department of Chemical Science and Technology, Faculty of Engineering, Kyushu University, 6-10-1 Hakozaki, Higashi-ku, Fukuoka 812, Japan*

(Received 1 September 1997; In final form 7 November 1997)

A drastic change from a transparent smectic-A (SmA) phase to a light-scattering chiral nematic (N^*) one is achieved in [side chain smectic-A liquid crystalline polymer (SCSmALCP)/low molecular weight nematic liquid crystal (LMWNLC)/chiral dopant] a ternary composite system with a homeotropic boundary condition. The light-scattering state of the induced N^* phase can be resumed into the initially transparent SmA phase on cooling slowly, and be frozen in the SmA phase on cooling rapidly. The effects of the composition of the ternary composite system on such thermo-optical characteristics are investigated.

Keywords: Smectic-A phase; chiral nematic phase; phase transition; thermo-optical characteristics; a homeotropic boundary condition

INTRODUCTION

It is well known that a homeotropically aligned smectic-A (SmA) liquid crystal (LC) prefers to orient the layers and its optical axis in the directions parallel and perpendicular to the substrate surfaces of the cell sandwiching

* Corresponding author.

the SmALC, respectively. This texture is very uniform and scatters little light. Therefore, the SmA phase is transparent. However, if the SmA phase is heated to the isotropic (I) phase and then cooled rapidly, the texture of the SmALC is unaligned, with the smectic planes oriented in different directions in different parts. Thus, a focal conic texture which strongly scatters light forms. If the focal conic texture is heated to the I phase and then cooled on application of an electric field, the focal conic texture will be erased and a homeotropic SmA phase forms again. Based on this principle, a thermal-addressing liquid crystal display (TALCD) mode using a LMWSmALC with a positive dielectric anisotropy is achieved [1, 2]. For practical use, a LMWSmALC in which there exists a narrow N phase or a narrow N* phase between the SmA phase and the I one, i.e. a LMWSmALC with SmA $\leftrightarrow$ N (or N*) $\leftrightarrow$ I phase transitions, should be used (Since the N or N* range is narrow, the LMWLC is still called LMWSmALC). This is because the homeotropically aligned SmA phase forms with difficulty on cooling even on application of an electric field if there is no narrow N (or N*) phase [3]. Since the focal conic texture of the SmA phase of a LMWSmALC with SmA $\leftrightarrow$ N* $\leftrightarrow$ I phase transitions formed on cooling rapidly from the I phase shows much stronger light scattering than that of a LMWSmALC with SmA$\leftrightarrow$N $\leftrightarrow$ I phase transitions, sometimes it is the former but not the latter that is used [4]. Thus, the process of a light-scattering texture induced from a transparent SmA phase is based on SmA $\rightarrow$ N(N*) $\rightarrow$ I$\rightarrow$N(N*) $\rightarrow$ SmA phase transitions.

Now it is not mysterious that SmA $\leftrightarrow$ N* phase transitions are rather sharp [5]. It will surely have great practical significance if the SmA and N* phases with a homeotropic boundary condition can show transparent and strong light scattering, respectively. Thus, a drastic change from a transparent SmA phase to a strong light-scattering N* one will be achieved accompanied by the sharp heat-induced SmA $\rightarrow$ N* phase transition. However, in fact, it is impossible for a LMWLC with SmA $\leftrightarrow$ N* phase transitions. It has been proved that the heat-induced N* phase of the LMWLC from the SmA one with a homeotropic boundary condition has a rather low intensity of light scattering, which was shown clearly in some experiments, [4, 6–8]. This is because it is a scroll texture, not a facol conic one that forms when a LMWN*LC is sandwiched between a cell with a homeotropic boundary condition [9–11]. Professor S. Kobayashi maintains that:

(a) If the gap of the cell to the pitch length of the sandwiched LMWN*LC is greater than 1/4, the LMWN*LC has a tendency to form a planar

conformation. This is due to the fact that a larger thermal fluctuation is allowed if the system takes a planar conformation, where the helical axis is vertical to the substrate surfaces, as opposed to the case where the helical axis is parallel to the substrate surfaces (focal conic texture).

(b) Due to homeotropic boundary condition of the cell, in the interfacial region of the cell the mesogenic molecules always take vertical alignment.

By combining (a) and (b), the formation of a scroll texture is expected [11, 12]. Therefore, when a LMWN*LC is sandwiched between a cell with a homeotropic boundary condition, the light-scattering intensity is very low because of the formation of the scroll texture.

Therefore there is little practical significance for the drastic change from the SmA phase to the N* one in a LMWLC with SmA $\leftrightarrow$ N* phase transitions with a homeotropic boundary condition due to the fact the contrast between the two phases is very low.

Since thermotropic SCLCPs exhibit both inherent mesomorphic properties of a LMWLC and the excellent mechanical characteristics of a polymer, SCLCPs have attracted great attention due to their promising applications as electro-optical devices [13]. However, since SCLCPs in a mesophase state are more viscous than LMWLCs, a (SCLCP/LMWLC) mixture in which the LMWLC takes the role of solvent or dilution to the SCLCP to reduce the magnitude of the viscosity of the SCLCP has attracted much more interest [14, 15]. Meanwhile, it has been found that a (SCLCP/LMWLC) mixture has some unique characteristics which don't exist in a pure LCP or a LC [16–19]. Moreover, it is demonstrated recently that, since the backbones of SCSmALCP of (SCSmALCP/LMWNLC/chiral dopant) ternary composites tend to adopt a random-coil statistical conformation in the N* phase, the directions of the helical axes of the small domains in the N* phase tend to distribute randomly when the ternary composite is sandwiched between a cell with a homeotropic boundary condition. Then a focal conic texture, not a scroll texture is formed in the N* phase of the (SCSmALCP/LMWNLC/chiral dopant) ternary composite and the N* phase shows strong light-scattering. Thus, a drastic change from a transparent state to a strong light-scattering one has been realized in the ternary composite based on the sharp SmA$\rightarrow$N* phase transition [8].

In this paper, the effects of the composition of the (SCSmALCP/LMWNLC/chiral dopant) ternary composite system on its thermo-optical characteristics will be studied.

EXPERIMENTAL

Materials

A SCSmALCP denoted as PS(4BC/DM), a commercially available LMWNLC, E7 (Merck Co., Ltd.), and a commercially available chiral compound, CB-15 (Merck Co., Ltd.), were used as the three components of the (SCSmALCP/LMWNLC/chiral dopant) ternary composite system. PS(4BC/DM) was synthesized following the method proposed by Finkelmann *et al.* [20] The purity and molecular weights of PS(4BC/DM) were evaluated by GPC, and the block ratio determined by NMR and FT-IR. The chemical structures and some physical parameters of these materials are shown in Figure 1. The [PS(4BC/DM)/E7/CB-15] ternary composite system was prepared by a solvent evaporation method from acetone solutions.

Fabrication of the Cells

The inner surfaces of ITO substrates of the cells were homeotropically treated with the method proposed by F. J. Kahn [21]. 14 μm-thick PET films were used as the spacers of the cells and the studied samples were put into the cells by the capillary action in their I phases.

Measurements

The phase transition temperatures and the aggregation structures of the studied samples were investigated on the basis of differential scanning

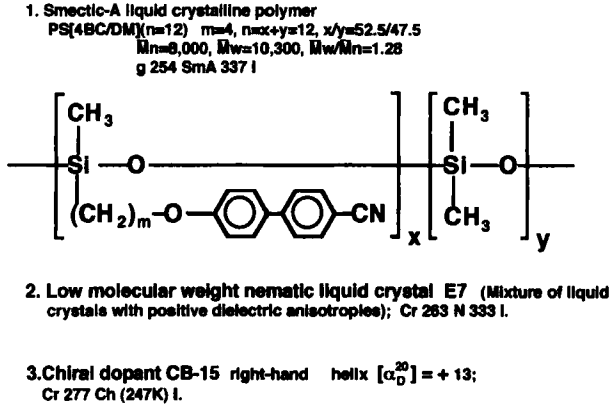

FIGURE 1 The chemical structures and some physical parameters of the materials used.

calorimeter (DSC) measurements, polarizing optical microscopy (POM) observation, and wide angle X-ray diffraction (WAXD) and small angle X-ray scattering (SAXS) studies. DSC thermograms were obtained by using a Rigaku DSC 8230B at a heating rate of 5.0 K min^{-1} under the protection of dry nitrogen purge, POM observation done under crossed nicols using a Nikon polaring optical microscope equipped with a hot stage calibrated to an accuracy of $\pm$ 0.05 K, and WAXD and SAXS studies carried out using Ni-filtered Cu Kα ($\lambda = 0.15405$ nm) radiation from a M18XHF (Macroscience Co., Ltd.) and a RU-300 (Rigaku) X-ray generator, respectively.

The Cano-Wedge technique [22] was used to measure the pitch lengths of the N^* phases of the studied samples and rubbed poly(vinylalcohol) (PVA) films were used to obtain the planar alignments.

The thermo-optical characteristics of the studied samples were investigated with the instrument as schematically shown in Figure 2. The direct beam of a He-Ne laser (2 mW, 632.8 nm) was used as the incident light and the measured data were recorded with a photodiode. The transmittance of a blank cell was taken as 100%.

RESULTS AND DISCUSSION

Phase Transition Behaviour and Aggregation Structures of [PS(4BC/DM)/E7/CB-15] Ternary Composite Systems

On the basis of DSC measurements, POM observation, WAXD and SAXS studies, the phase diagrams of three [PS(4BC/DM)/E7/CB-15] ternary composite systems denoted as systems 1, 2 and 3, in which CB-15 ratios were 2.4 wt%, 4.8 wt% and 9.1 wt%, were determined and are shown in Figures 3, 4 and 5, respectively. From these three figures, the following can be observed:

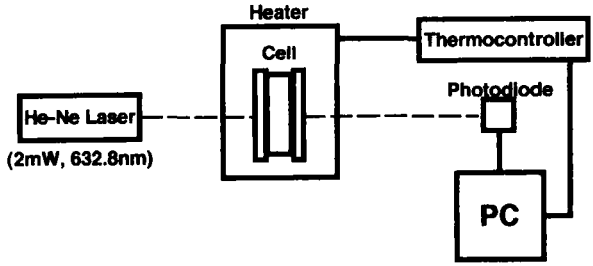

FIGURE 2 The schematic representation of the instrument used to measure the thermo-optical characteristics of samples.

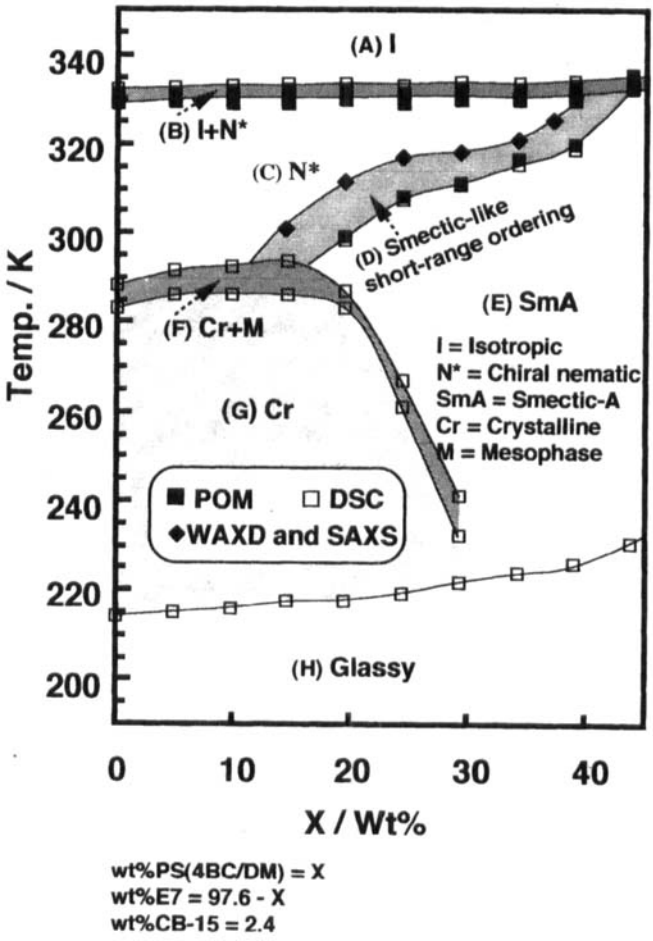

FIGURE 3 The phase diagram of system 1.

(a) Since the $N^* \rightarrow I$ phase transition temperatures of PS(4BC/DM) and E7 were very near, the $N^* \rightarrow I$ phase transition temperatures of each system changed little with the PS(4BC/DM) ratio. Comparing systems 1, 2 and 3 with each another, it becomes clear that the $N^* \rightarrow I$ phase transition temperature of the ternary composite system decreased with increasing the CB-15 ratio. Obviously, the thermal stability of the N^* of the ternary composite system decreased with increasing the CB-15 ratio since CB-15 was a non-mesogenic compound.

(b) The crystalline (Cr) $\rightarrow$ mesophase (N^* or SmA) phase transition temperature of each system decreased on the whole with increasing the PS(4BC/DM) ratio. This should result from the backbones of

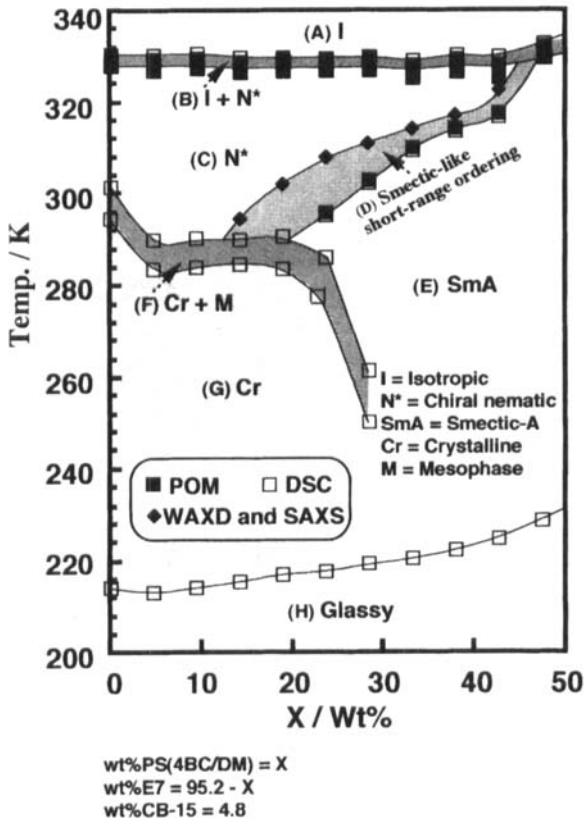

FIGURE 4 The phase diagram of system 2.

PS(4BC/DM) tending to have a restricting effect on the formation of the crystalline structure due to the backbones tending to adopt a random-coil statistical conformation. Comparing systems 1, 2 and 3 with each another, it becomes clear that, if the relative ratio of PS(4BC/DM)/E7 was unchanged, the phase transition temperature tended to decrease with increasing the CB-15 ratio since the greater ratio of CB-15 tended to cause more crystal defects in the crystalline structure and decrease the thermal stability of the crystalline phase.

(c) The glass transition temperature of each system decreased with increasing the E7 ratio. This was obviously due to the well-known "softening effect". Meanwhile, comparing systems 1, 2 and 3 with each another, it becomes clear that, if the relative ratio of PS (4BC/DM)/E7 is the same, the glass transition temperature tended to decrease with

increasing the CB-15 ratio. This should be due to the mesogenic interaction between the mesogenic molecules decreasing with increasing the CB-15 ratio. Then the restricting effect of the mesogenic molecules on the motion of the backbones decreased. Therefore, the motion of the backbones became easier with increasing the CB-15 ratio. Thus, the glass transition temperature decreased a little with increasing the CB-15 ratio.

(d) A SmA phase existed below the temperature range of a N^* one in each system when the PS(4BC/DM) ratio was 14.6 wt% and 43.9 wt% for system 1, between 19.1 wt% and 47.6 wt% for system 2, and between 22.7 wt% and 50.0 wt% for system 3, respectively. In each system, the SmA $\rightarrow$ N^* phase transition temperature increased with increasing the PS(4BC/DM) ratio. After comparing systems 1, 2 and 3 with each another, it was known that: the same as the $N^* \rightarrow I$ phase transition temperature, the SmA$\rightarrow$ N^* phase transition temperature decreased somewhat with increasing the CB-15 ratio if the relative ratio of PS(4BC/DM)/E7 was unchanged.

(e) X-ray studies proved that, in each ternary composite system, smectic-like short-range ordering existed in a certain temperature range just above the SmA $\rightarrow$ N^* phase transition and increased as temperature dropped to near the SmA $\rightarrow$ N^* phase transition temperature. Moreover, the temperature range of smectic-like short-range ordering became wider as the width of the N^* phase increased. This is to be expected since the SmA$\rightarrow N^*$ phase transition is always becoming more of a second order as the N^* range increases [23]. It should be mentioned here that smectic-like short-range ordering was not different in any macroscopic sense from the N^* phase; the only difference was at a local molecular level and so there was no true boundary between the regions of the existence of smectic-like short-range ordering and the N^* phase. The boundaries shown in Figures $3 \sim 5$ were just to show the region of the existence of smectic-like short-range ordering approximately.

Table I lists the composition of the samples 1A$\sim$3D. And Figure 6 shows the temperature dependences of pitch lengths of the N^* phases of samples 1A $\sim$ 3D. It is shown in Figure 6 that the pitch lengths of the N^* phases of all samples varied only a little with temperature. This can't be explained because, up to now, some order parameters necessary to explain the temperature dependence of the pitch length of an N^* phase can not be obtained yet [24]. For each system, the pitch length tended to increase with increasing the PS(4BC/DM) ratio. Finkelmann maintains that, when only

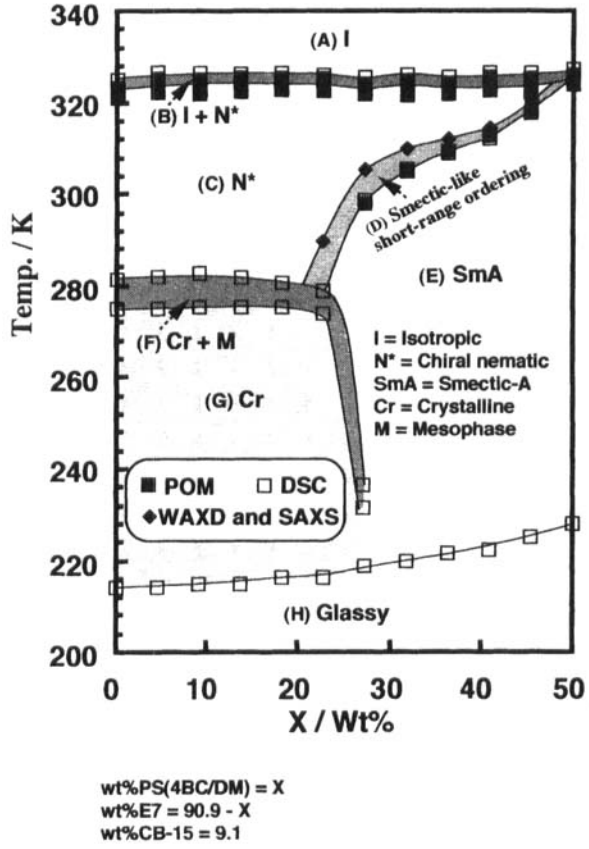

FIGURE 5 The phase diagram of system 3.

molecular biaxiality is considered, the pitch length of an N* phase was determined by two order parameters S and D [25]

$$S = \frac{1}{2}\left\langle 3\cos^2\theta - 1 \right\rangle$$

$$D = \left\langle \cos 2\Psi \sin^2\theta \right\rangle$$

where θ is the angle between the long axis of a molecule and the director of the mesophase and Ψ is the angle of the rotation of a mesogenic molecule around its long axis. Since the rotation of the side mesogenic groups around their long axes was hindered somewhat by the backbones, the order parameter D of the ternary composite system should increase with increasing the PS(4BC/DM) ratio. Thus, the pitch length of the N* phase

TABLE I The ratios of PS(4BC/DM)/E7/CB-15 of samples 1A ~ 3D and the thicknesses of the spacers of the corresponding cells sandwiching these samples

Sample	*System* 1				*System* 2				*System* 3			
	1*A*	1*B*	1*C*	1*D*	2*A*	2*B*	2*C*	2*D*	3*A*	3*B*	3*C*	3*D*
Ratio/wt%	19.5/78.1/ 2.4	24.4/73.2/ 2.4	29.3/68.3/ 2.4	34.2/63.4/ 2.4	23.8/71.4/ 4.8	28.6/66.6/ 4.8	33.3/61.9/ 4.8	38.1/57.1/ 4.8	27.3/63.6/ 9.1	31.8/59.1/ 9.1	36.4/54.5/ 9.1	40.9/50.0/ 9.1
Thickness/μm	14	17	16	16	23	20	18	17	18	21	14	15

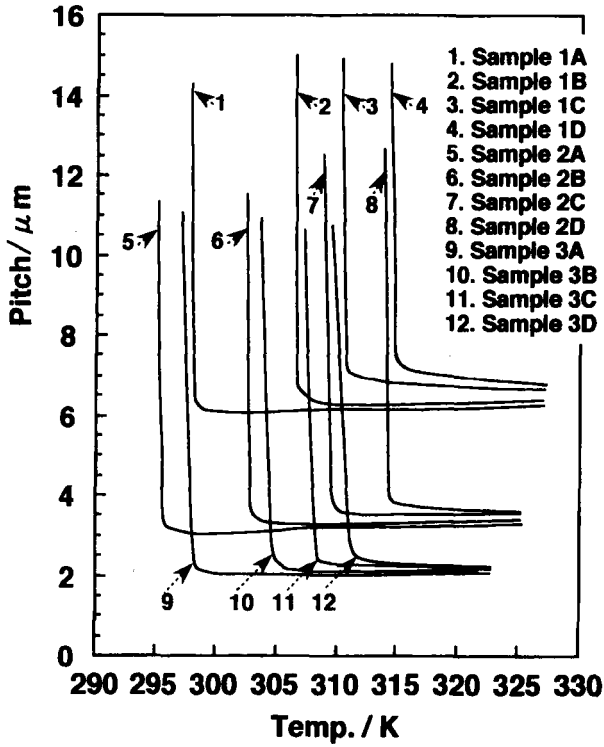

FIGURE 6 The representation of the temperature dependence of the pitch lengths of the N* phases of samples 1A~3D, respectively.

of the ternary composite system should decrease with increasing the PS(4BC/DM) ratio. However, it is shown in Figure 6 that the pitch length of the N* phase of each system increased with increasing the PS(4BC/DM) ratio. Therefore, it must be that the order parameter S had decreased with increasing the PS(4BC/DM) ratio, and obviously the variation of the order parameter S had a greater effect on the pitch length than the variation of the order parameter D with increasing the PS(4BC/DM) ratio. This was not a strange result. It has been proven by Piskunov *et al.*, that, if the chemical structure of the side mesogenic groups of a SCN*LCP is similar to that of the mesogenic molecules of a LMWN*LC, the order parameter S of the former is somewhat lower than that of the latter since the backbones of the SCN*LCP tended to adopt a random-coil statistical conformation in the mesophase [26]. Therefore, the order parameter S of the ternary composite system should decrease with increasing the PS(4BC/DM) ratio and then the

pitch length of the N* phase of each system increased somewhat with increasing the PS (4BC/DM) ratio. It is also shown in Figure 6 that the pitch lengths of the N* phases of the samples of system 2 were smaller than those of the samples of system 1, and the pitch lengths of the samples of system 3 were smaller than those of the samples of system 2. This should be because the helical twisting power of the ternary system increased somewhat with increasing the CB-15 ratio.

The phenomenon of critical divergence of a pitch, i.e. a drastic change in the pitch from a certain value to infinity accompanied with the N* → SmA phase transition, existed in each sample in the cooling process [5]. Qualitatively, this phenomenon can be understood as follows: Due to the relative high rigidity, it was difficult for the layer structure of a SmA phase to buckle in order to twist. On cooling from an N* phase and near the N* → SmA phase transition temperature, smectic-like short-range ordering started to form in the N* phase, and some groups of molecules began to show some fleeting layer structure. As the temperature dropped closer to the transition temperature, smectic-like short-range ordering increased further and more molecules tended to arrange themselves in layers. This resulted in the increase in twisting elastic constant K_{22}, and made it increasingly difficult for the N* phase to twist. Then the pitch lengthened. Since all this could only take place very near the N* → SmA phase transition temperature, the pitch change happened within a tiny temperature range. Thus, the phenomenon of critical divergence of the pitch occured. POM observation had demonstrated that the critical convergence of the pitch, i.e. a drastic change in the pitch from infinity to a certain value accompanied the SmA → N* phase transition and also existed in each sample in the heating process. These indicate that the SmA ↔ N* phase transitions of these samples were sharp.

Thermo-optical Characteristics of [PS(4BC/DM)/E7/CB-15] Ternary Composite Systems Based on SmA → N* Phase Transitions

Figures 7a ~ 7d, 8a ~ 8d show the temperature dependence of the transmittances of the cells sandwiching samples 1A ~ 1D and 2A ~ 2D. Since the inner surfaces of each cell were treated homeotropically, the SmA phase of each sample oriented the optical axis in the direction perpendicular to the substrate surfaces in a single-crystal manner by the anchoring effect of the surfacial orientation agent. Therefore the SmA phase of each sample was transparent as shown in the figures. When each cell was heated at a rate of 10.0 K min^{-1} or 30.0 K min^{-1} (curves 1 and 2), a change from a transparent

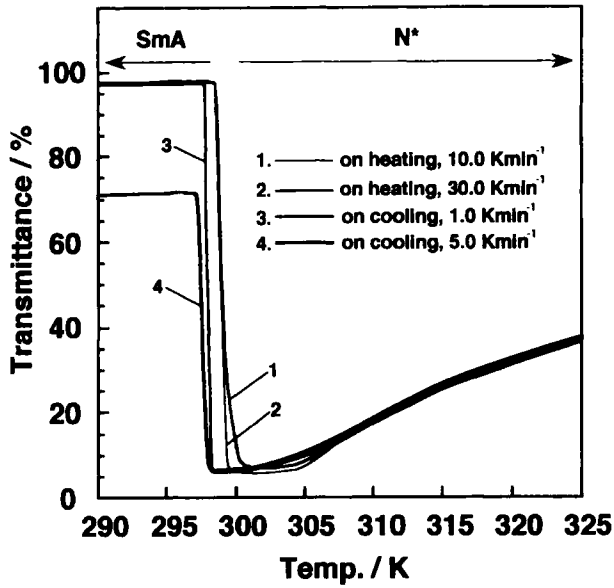

FIGURE 7a The representation of the temperature dependence of the transmittance of the cell sandwiching sample 1A.

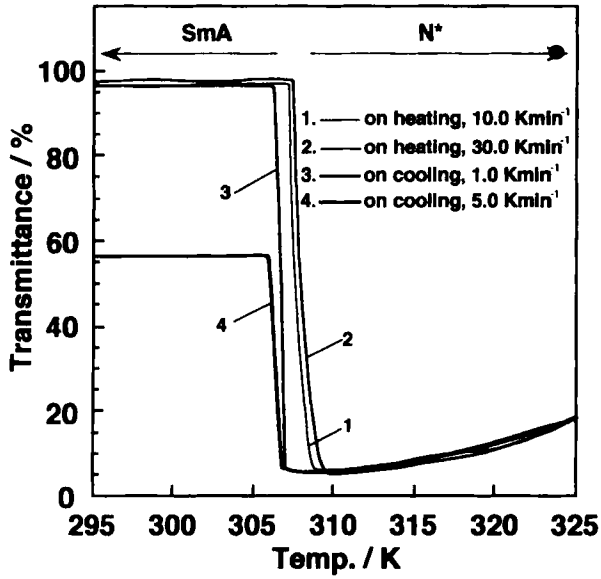

FIGURE 7b The representation of the temperature dependence of the transmittance of the cell sandwiching sample 1B.

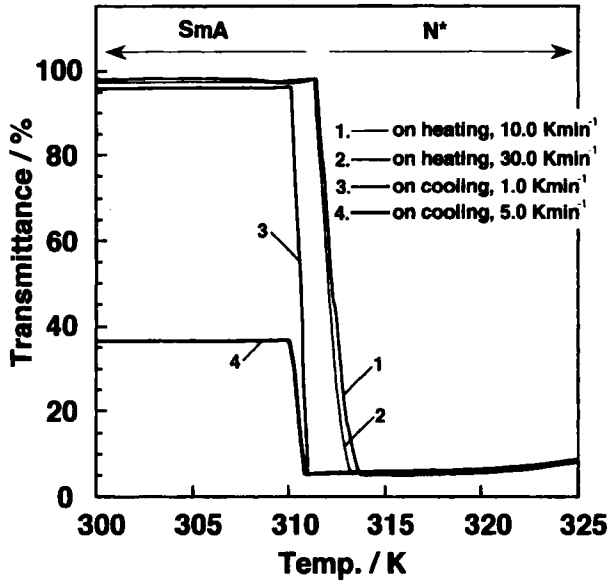

FIGURE 7c The representation of the temperature dependence of the transmittance of the cell sandwiching sample 1C.

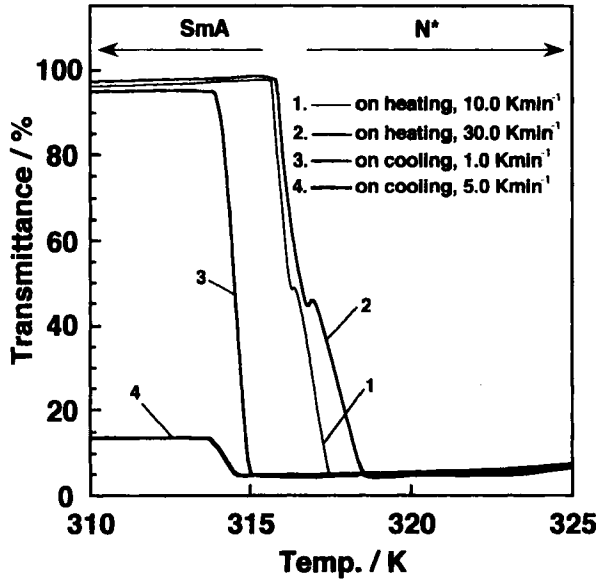

FIGURE 7d The representation of the temperature dependence of the transmittance of the cell sandwiching sample 1D.

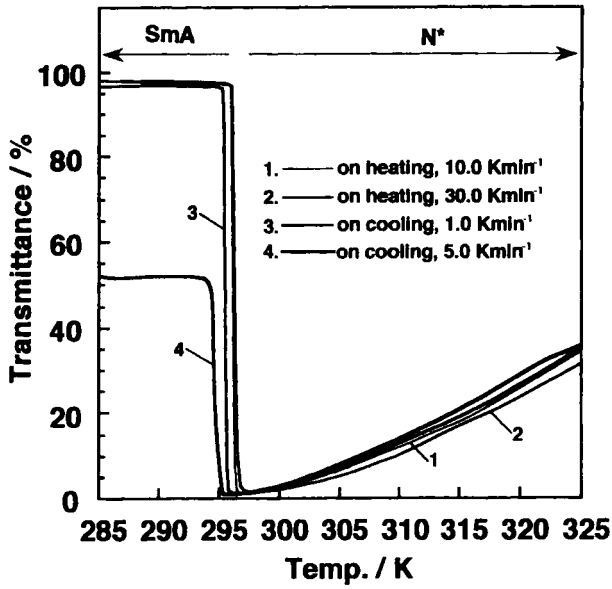

FIGURE 8a The representation of the temperature dependence of the transmittance of the cell sandwiching sample 2A.

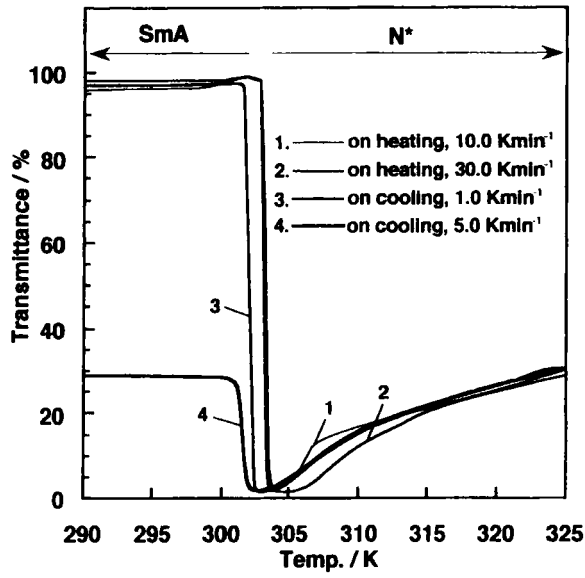

FIGURE 8b The representation of the temperature dependence of the transmittance of the cell sandwiching sample 2B.

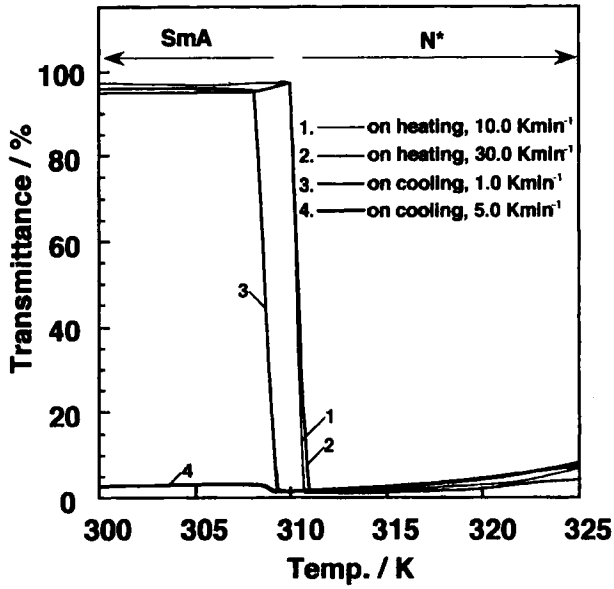

FIGURE 8c The representation of the temperature dependence of the transmittance of the cell sandwiching sample 2C.

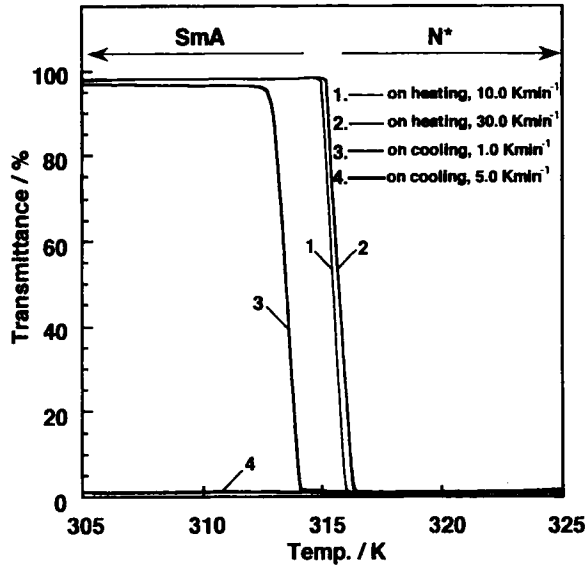

FIGURE 8d The representation of the temperature dependence of the transmittance of the cell sandwiching sample 2D.

state to a light-scattering one occurred accompanied by the heat-induced SmA $\rightarrow$ N* phase transition. In the initial stage of the formation of the N* phases of samples 1A (Fig. 7a), 1B (Fig. 7b), 2A (Fig. 8a) and 2B (Fig. 8b), these N* phases showed very strong light scattering. This indicates that a focal-conic texture had formed in the induced N* phase of each of these samples in the initial stage of the formation of the N* phase. This was quite different from a LMWLC with SmA $\leftrightarrow$ N* $\leftrightarrow$ I phase transitions sandwiched between a cell with a homeotropic boundary condition, in which the N* phase showed very low light scattering, i.e. a scroll texture formed in the N* phase, even in the initial stage of the formation of the N* phase [6–8]. One of the reasons that a scroll texture didn't form in the initial stage of the formation of the N* phase of each of the above samples might be that the backbones of PS (4BC/DM) which tended to adopt a random-coil statistical conformation tended to make the directions of the helical axes of the small domains in the N* phase distributed randomly. The other might be that the bend elastic constant, K_{33}, of the N* phase in the initial stage of the formation of the N* phase was very great since smectic-like short-range ordering existed. And then, it should be a focal conic texture not a scroll texture that formed more easily, affected by the anchoring effect of the surfacial orientation agent. It has already been proven that the existence of smectic-like short-range ordering makes an N* phase tend to adopt a focal-conic texture [27]. Thus, based on the above two reasons, it was a focal-conic texture, not a scroll texture that had formed in the N* phases of samples 1A, 1B, 2A and 2B in the initial stage of the formation of N* phases. Therefore the N* phases showed strong light scattering in the initial stage of the formation of the N* phases. Since, on one hand, the anchoring effect of the surfacial orientation agent coated onto the inner surfaces of the substrates on mesogenic molecules decreased with increasing temperature due to the bend elastic constant, K_{33}, always decreasing with increasing temperature, and on the other hand a scroll texture was a in more stable state when an N* phase was sandwiched between a cell with a homeotropic boundary condition, the directions of some domains in the cell tended to rotate to be perpendicular to the substrate surfaces with increasing temperature. Then the light-scattering intensity of the induced N* phase of each of samples 1A, 1B, 2A and 2B decreased with increasing temperature.

It is shown in Figures 7c, 7d, 8c and 8d that the N* phases of samples 1C, 1D, 2C and 2D showed strong light scattering in all their temperature ranges. This should result from the higher ratio of PS(4BC/DM) in these samples. Since the backbones of PS(4BC/DM) which tended to adopt a

random-coil statistical conformation had a restricting effect on the formation of a scroll texture, and N* phase with strong and stable light scattering, i.e. the formation of a focal-conic texture, in all the temperature ranges of the N* phase should be obtainable if the PS(4BC/DM) ratio is high enough in the sample. Therefore, the N* phases of samples 1C, 1D, 2C and 2D showed strong light scattering in all their temperature ranges. Thus, a change from a transparent state to a strongly light-scattering one was achieved in samples 1C, 1D, 2C and 2D as shown in Figures 7c, 7d, 8c and 8d. In addition, after observing Figures 7a ~ 7d and 8a ~ 8d carefully, it is found that for samples with the same relative ratio of PS(4BC/DM)/E7, the minima of transmittances of the N* phases of the samples of system 1 were, on the whole, somewhat greater than those of system 2. This should be attributed to the longer pitches of the samples of system 1 than those of the samples of system 2.

Figures 9a ~ 9c showed the temperature dependence of the transmittances of the cells sandwiching samples 3C~3D. Since CB-15 was a non-mesogenic compound and the interaction between the mesogenic molecules decreased with increasing the CB-15 ratio, the fluctuation of the homeotropic orientation of the SmA phase should increase with increasing the CB-15 ratio. Therefore the transmittances of the SmA phases of samples 3C~3D

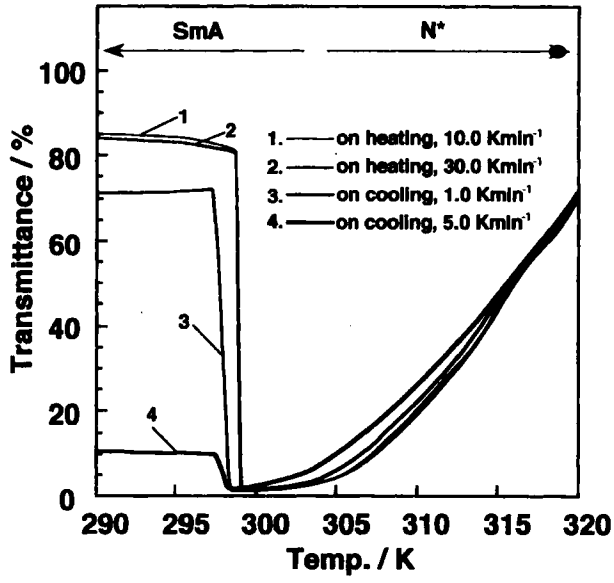

FIGURE 9a The representation of the temperature dependence of the transmittance of the cell sandwiching sample 3A.

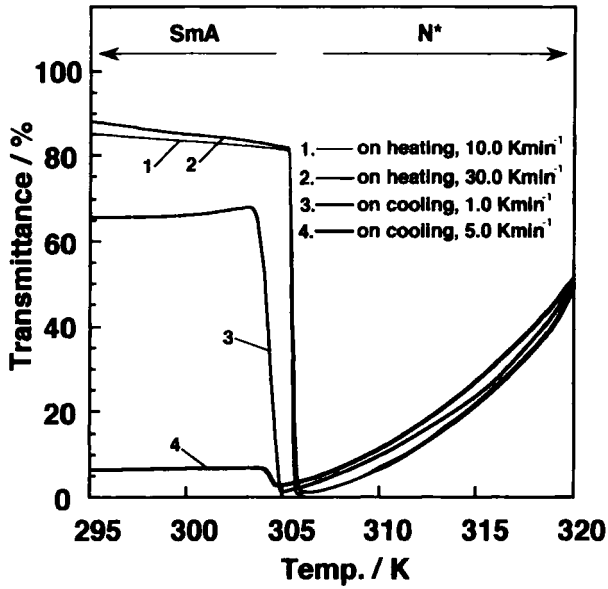

FIGURE 9b The representation of the temperature dependence of the transmittance of the cell sandwiching sample 3B.

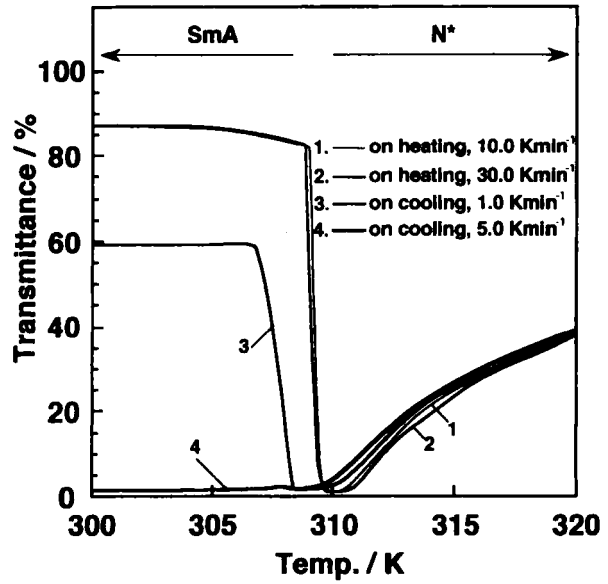

FIGURE 9c The representation of the temperature dependence of the transmittance of the cell sandwiching sample 3C.

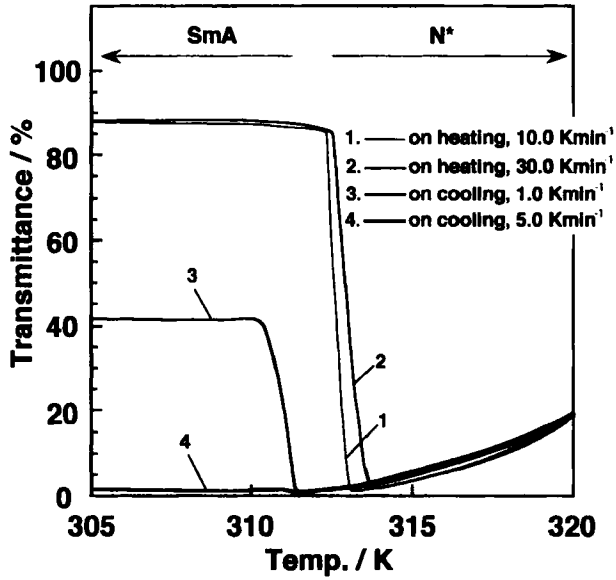

FIGURE 9d The representation of the temperature dependence of the transmittance of the cell sandwiching sample 3D.

were somewhat lower than those of the SmA phases of the samples of systems 1 and 2. As with the samples of systems 1 and 2, a change from a transparent SmA phase to a light-scattering one accompanied by the SmA→ N* phase transition also occurred in each of samples 3C~3D. Moreover, the tendency of the light-scattering intensity of the N* phase to decrease with increasing temperature in samples 3C ~ 3D also decreased with increasing the PS(4BC/DM) ratio. However, although the relative ratio of PS(4BC/DM)/E7 in sample 3D was much greater than those in samples 1C, 1D, 2C and 2D, the light-scattering intensity of the N* phase obviously still decreased with increasing temperature. This might be that a scroll texture formed more easily with increasing the ratio of the gap of the cell to the pitch length of the sandwiched sample [11], which will be investigated further.

Table II lists the response times of samples 1A~1D, 2A~2D and 3A~3D necessary for the changes in transmittances on going from 10.0% to 90.0% response from the transparent SmA phase to a light-scattering N* one on heating at rates of 10.0 K min^{-1} and 30.0 K min^{-1}, respectively. It becomes clear from Table II or from Figures 7a ~ 7d, 8a ~ 8d and 9a ~ 9d that the response time of each system increased with increasing the PS(4BC/DM) ratio on heating at a certain heating rate. This should be attributed to the

TABLE II The response times necessary for the drastic changes in transmittances on going from 10.0% to 9.0% response on heating at rates of 10.0 K min^{-1} and 30.0 K min^{-1}, respectively

Sample / *Time/s* / *Heating rate/K min^{-1}*	1A	1B	1C	1D	2A	2B	2C	2D	3A	3B	3C	3D
10.0	5.4	7.8	9.4	10.8	2.1	3.0	3.9	5.0	1.7	2.3	2.9	3.6
30.0	3.0	3.4	4.0	5.0	0.9	1.2	1.7	2.6	0.7	0.9	1.4	2.0
50.0	2.1	2.3	2.7	3.5	0.6	0.8	1.2	1.8	0.5	0.6	0.9	1.2

viscosity of the ternary composite system increased with increasing the PS(4BC/DM) ratio. Comparing samples 1C, 2B and 3A with each other or comparing samples 1D, 2C and 3B with each other, it becomes clear that, if the relative ratios of PS(4BC/DM)/E7 were the same, the response time decreased with increasing the CB-15 ratio. This should be because the helical twisting power increased with increasing the CB-15 ratio. For each sample, the response time of the change decreased with increasing the heating rate. By the way, the temperature intervals for the change from a transparent SmA phase to a light-scattering N* one were all smaller than 1.0 K for samples 2A~2D and 3A~3D when these samples were heated at a rate of 10.0 K min^{-1}. Therefore the changes in these samples were drastic.

It is shown in Figures 7a, 7b, 8a and 8b that, since the K_{33} of the N* phase increased and the thermal fluctuation in each sample decreased with decreasing temperature, the light-scattering intensity of the N* phases of samples 1A, 1B, 2A and 2B increased somewhat with decreasing temperature affected by the anchoring effect of the surfacial orientation agent (curves 3 and 4). Moreover, on cooling at a rate of 1.0 K min^{-1}, the initially transparent SmA phase of each of samples 1A ~ 1D and 2A ~ 2D was resumed, accompanied with the phenomenon of critical divergence of the pitch affected by the anchoring effect of the surfacial orientation agent. However, the transmittance of the resulting SmA phase obtained on cooling from the N* phase at a rate 5.0 K min^{-1} in each samples was lower than that of the SmA phase obtained on cooling at a rate of 1.0 K min^{-1}. This is obviously because the molecules were frozen in the higher viscous SmA phase before the molecules had rearranged from a N* phase into a homeotropic SmA phase completely due to the more rapid cooling. Furthermore, it becomes clear from Figures 7a ~ 7d or 8a ~ 8d that the initially transparent SmA phase of the samples of either system 1 or system 2 tended to resume more easily with decreasing the PS(4BC/DM) ratio when cooled from the N* phase at a rate of 5.0 K min^{-1}. This might be because of the following two reasons. One was that, N* → SmA phase transition of

either system was becoming more second-order in character as the N* range increased. Then, the twist and the bend elastic constants of the N* phase tended to disperse during N* → SmA phase transition with increasing N* range. Therefore, the transmittance of the SmA phase obtained on cooling at a certain rate tended to be greater as the N* range increased [5, 23]. The other was that the viscosity of the system decreased as the PS(4BC/DM) ratio decreased. This means that the rearrangement of the mesogenic molecules from an N* phase to a homeotropic SmA one needed shorter time with decreasing the PS (4BC/DM) ratio and then the light-scattering state of the N* phase became frozen with more difficulty in the SmA phase. Based on these two reasons, the initially transparent SmA phase of system 1 or 2 tended to resume more easily with the PS(4BC/DM) ratio decreasing when cooled from the N* phase at a rate of 5.0 K min^{-1}.

The patterns of curves of the dependence of the transmittances of the samples of system 3 measured on cooling as shown in Figures 9a ~ 9d are similar to those of the samples of systems 1 and 2. Comparing samples 2B (Fig. 8b) with 3A (Fig. 9b) or comparing samples 2C (Fig. 8c) with 3B (Fig. 9b), it becomes clear that, if the relative ratios of PS(4BC/DM)/E7 were the same, the light-scattering state of the N* phase became frozen more easily in the SmA phase on cooling at a certain rate with increasing the CB-15 ratio. This should be because the helical twisting power increased with increasing the CB-15 ratio. It has been proven that the twist force of a chiral dopant can greatly improve the light-scattering intensity of an SmA phase obtained on cooling from an N* phase [4]. Therefore the transparent SmA phases of the samples of system 3 couldn't be resumed completely even if these samples were cooled at a rate of 1.0 K min^{-1}.

It is shown in Figures 7a ~ 7d, 8a ~ 8d or 9a ~ 9d that, similar to most phase transitions in organic compounds, thermal hysteresis at the N*→ SmA phase transition appeared in each sample and increased a little with increasing the cooling rate. Furthermore, the thermal hysteresis at the N*→ SmA phase transition of each of systems 1, 2 and 3 decreased as the N* range increased. This is also because the N*→ SmA phase transition was becoming more second-order as the N* range increased.

CONCLUSION

From the above discussion, it becomes clear that a drastic change from a transparent SmA phase to a light-scattering N* one can be induced in the [PS(4BC/DM)/E7/CB-15] ternary composite system accompanied by the

SmA → N* phase transition. The light-scattering state of the N* phase will be transformed into a transparent SmA phase on cooling slowly and frozen in the SmA phase on cooling rapidly. With increasing the PS(4BC/DM) ratio, a focal-conic texture which shows strong light scattering becomes easier to form in all the temperature ranges of the N* phase, the response time of the drastic change increases, and the light scattering state of the N* phase is frozen more easily in the SmA phase on cooling rapidly. With increasing the CB-15 ratio, the light-scattering intensity of the N* phase increase in the range of the lower CB-15 ratio while the tendency of the formation of a scroll-like texture in the N* phase increases in the range of the higher CB-15, the response time of the drastic change decreases, and the light scattering state of the N* phase is frozen more easily in the SmA phase on cooling rapidly. Based on these characteristics, it is most possible that the [PS(4BC/DM)/E7/CB-15] ternary composite system will be used as a sensitive thermo-optical sensor, or the [PS(4BC/DM)/E7/CB-15] ternary compostie will be used as a novel thermal-addressing liquid crystal display material based on the SmA ↔ N* phase transitions, different form the currently used LMWSmALCs based on the SmA ↔ N(N*) ↔ I phase transitions. Furthermore, the desired application can be designed and optimized by adjusting the composition of the ternary composite system.

Some explanations in this paper are somewhat speculative and further study will also be carried out.

Acknowledgement

The authors are indebted to professor S. Kobayashi for very much valuable advice on the formation of a scroll texture.

References

[1] S. Le Berre, M. Hareng, R. Hehlen and J. N. Perbet, *SID '82 Int. Symp.*, 252 (1982).
[2] D. H. Davies and S. Lu, *Mol. Cryst. Liq. Cryst.*, **94**, 167 (1983).
[3] The 142nd Committee of Japanese Scientific Promotion Society, Ed., *Handbook of Liquid Crystals* (in Japanese), Industrial Daily Press, p. 376 (1989).
[4] H. Hatoh, *Mol. Cryst. Liq. Cryst.*, **250**, 1 (1994).
[5] T. C. Lubensky, *J. de Physique*, **36**, Cl-151 (1975).
[6] A. Sasaki, K. Kurahashi and T. Takagi, *J. Appl. Phys.*, **45**, 4356 (1974).
[7] O. Kouji and S. Kobayashi, *Liquid Crystal* [Appication Section] (in Japanese), Tutikafuu Kann, p. 44 (1985).
[8] Yang Huai, Hirokazu Yamane, Hirotsugu Kikuchi and Tisato Kajiyama, submitted to *Makromol. Chem., Rapid Commun.*
[9] R. A. Kashnow, J. E. Bigelow, H. S. Cole and C. R. Stein, *Liquid Crystal and Ordered Fluids*, Eds., J. F. Johnson and R. S. Porter, Plenum Press, Inc., New York, **2**, p. 483 (1974).

[10] M. Kawachi, K. Kato and O. Kogure, *Japan J. Appl. Phys.*, **16**(7), 1263 (1977).
[11] O. Kouji and S. Kobayashi, *Liquid Crystal* [Application Section] (in Japanese), p. 37 and 56, Tutikafuu Kann (1985).
[12] Private letter.
[13] C. B. McArdle, Ed., "*Side Chain Liquid Crystal Polymers*", Chapman and Hall, Inc., New York, N. Y. (1989).
[14] T. Kajiyama, H. Kikuchi, A. Miyamoto, S. Moritomi and J. C. Hwang, *Chem. Lett.*, 817 (1989).
[15] H. Kikuchi, J. C. Hwang and T. Kajiyama, *Polym. Adv. Technol.*, **1**, 297 (1991).
[16] T. Kajiyama, H. Kikuchi, A. Miyamoto, S. Moritomi and J. C. Hwang, *Mater. Res. Soc. Sym. Proc.*, **171**, 305 (1990).
[17] T. Kajiyama, H. Kikuchi, J. C. Hwang, A. Miyamoto, S. Moritomi and Y. Morimura, *Prog. in Pacific Polym. Sci.*, **1**, 343 (1991).
[18] J. C. Hwang, H. Kikuchi and T. Kajiyama, *Polymer*, **33**, 1821 (1992).
[19] H. Kikuchi, S. Kibe and T. Kajiyama, *SPIE*, **2408**, 141 (1995).
[20] H. Finkelmann, U. Kiechle and G. Rehage, *Mol. Cryst. Liq. Cryst.*, **94**, 343 (1983).
[21] F. J. Kahn, *Appl. Phys. Lett.*, **22**(8), 386 (1973).
[22] R. Cano, *Bull. Soc. Franc. Mineral.*, **91**, 20 (1968).
[23] P. E. Cladis and S. Torza, *J. Appl. Phys.*, **46**, 584 (1975).
[24] W. J. A. Goossens, *Appl. de. Physique*, **40**, C3-158 (1979).
[25] H. Finkelmann and G. Rehage, *Advances in Polymer Science*, **60/61**, Springer-Verlag Berlin Heidelberg, p. 99 (1984).
[26] M. Pishkunov, S. Kostromin, L. Stroganov, V. Shibaev and N. Plate, *Makromol. Chem. Rapid Commun.*, **3**, 443 (1982).
[27] C. B. McArdle, Ed., "*Side Chain Liquid Crystal Polymers*", Chapman and Hall. Inc., New York, N. Y., p. 273 (1989).